Crucial involvement of the CCL3-CCR5 axis-mediated fibroblast accumulation in colitis-associated carcinogenesis in mice

Crucial Involvement of the CCL3-CCR5 Axis-mediated Fibroblast Accumulation in Colitis-associated Carcinogenesis in Mice

Soichiro Sasaki,[1, 2] Tomohisa Baba,[1] Kei Shinagawa,[3] Kouji Matsushima,[2, 4] and Naofumi Mukaida[1,2]

[1]Division of Molecular Bioregulation, Cancer Research Institute, Kanazawa University, Kanazawa, Japan; [2]Japan Science and Technology Agency, Core Research for Evolutionary Science and Technology, Tokyo, Japan; [3]Department of Gastroenterology and Metabolism, Graduate School of Biomedical Sciences, Hiroshima University, Hiroshima, Japan; [4]Department of Molecular Preventive Medicine, Graduate School of Medicine, University of Tokyo, Tokyo, Japan

Short title: CCL3-CCR5 axis in colon carcinogenesis

Corresponding author: Naofumi Mukaida, MD, Ph.D.
Division of Molecular Bioregulation, Cancer Research Institute, Kanazawa University, Kakuma-machi, Kanazawa, Ishikawa 920-1192, Japan
TEL: +81-76-264-6735; Fax: +81-76-234-4520; Email: mukaida@staff.kanazawa-u.ac.jp

Keywords: colorectal cancer, CCL3, CCR5, fibroblast, HB-EGF
Category: Cancer Cell Biology

Novelty and Impact:

Colitis-associated cancer can be reproduced in mice by repeated oral ingestion of dextran sulfate sodium solution after intraperitoneal injection of azoxymethane. We provided the first definitive evidence to indicate that the CCL3-CCR5 axis-mediated fibroblast accumulation is required, in addition to leukocyte infiltration, to induce full-blown carcinogenesis in this model. Moreover, this process was blocked by an antagonist of CCR5, suggesting its therapeutic potential for cancers accompanied with fibroblast accumulation.

Abstract

Patients with inflammatory bowel diseases often develop colon carcinoma. Combined treatment of azoxymethane (AOM) and dextran sulfate sodium (DSS) recapitulates colitis-associated cancer in mice. AOM/DSS-induced tumor formation was reduced in *CCL3*- or its specific receptor, *CCR5*-deficient mice despite the presence of a massive infiltration of inflammatory cells. However, AOM/DSS-induced type I collagen-positive fibroblast accumulation in the colon was reduced in *CCL3*- or *CCR5*-deficient mice. This was associated with depressed expression of heparin-binding epidermal growth factor-like growth factor (HB-EGF), which is expressed mainly by fibroblasts. Moreover *in vitro*, CCL3 induced fibroblasts to proliferate and to enhance HB-EGF expression. Furthermore, CCR5 blockade reduced tumor formation together with reduced fibroblast accumulation and HB-EGF expression, even when administered after the development of multiple colon tumors. Thus, CCL3-CCR5-mediated fibroblast accumulation may be required, in addition to leukocyte infiltration, to induce full-blown colitis-associated carcinogenesis. This process can be blocked by a CCR5 antagonist, which may have therapeutic potential.

Introduction

Dvorak proposed that tumor is a wound that does not heal, based on the morphological changes shared between wound healing and tumor; consisting of leukocyte infiltration, neovascularization, and fibroblast accumulation (1). His hypothesis is corroborated by several lines of clinical and experimental evidence supporting the contribution of cancer-associated inflammation to tumor development and progression (2). One typical example is colitis-associated cancer (CAC), which ensues after chronic intestinal inflammation arising from inflammatory bowel disease (IBD) such as ulcerative colitis (UC) (3). Pathological features of UC are prolonged and uncontrolled inflammatory responses with prominent leukocyte infiltration in the colonic mucosa. These conditions frequently cause DNA damage with microsatellite instability in mucosal cells, and eventually can progress to cancer (4). Likewise, chronic inflammation can cause cancer in other organs, such as asbestosis-related mesothelioma and is estimated to account for nearly 20 % of cancer cases (2). Thus, the elucidation of chronic inflammation-associated carcinogenesis is important to develop novel therapeutic modalities for various types of cancer.

Oral administration of dextran sulfate sodium (DSS) to rodents can recapitulate the pathological changes of human UC (5). Moreover, repeated oral DSS ingestion can cause colon carcinoma (6) and this carcinogenesis process is promoted by prior administration of azoxymethane (AOM) (7), which causes O^6-methyl-guanine formation and induces mutations of the *β catenin* gene (8). Thus, combined treatment with AOM and DSS can reproduce CAC in rodents at morphological and molecular levels. We previously demonstrated that AOM/DSS-induced CAC is accompanied with massive leukocyte infiltration together with enhanced expression of several chemokines including CXCL1 and CCL2 (9). Moreover, CCL2 blockade decreased intracolonic macrophage infiltration, attenuated neovascularization, and eventually reduced the numbers and size of colon tumors, even when given after multiple colon tumors have developed (10). These

observations revealed an indispensable role of a chemokine, CCL2, in the initiation and progression of CAC.

Evidence is accumulating to indicate that cancer-associated fibroblasts (CAFs), the fibroblasts in tumor tissues, also have a crucial role in tumor development and progression (11). In the AOM/DSS-induced CAC model, the contribution of CAF-derived growth factors has been documented (12, 13). However, the mechanism regulating CAF trafficking in AOM/DSS-induced CAC remains unclear. We observed that AOM/DSS treatment enhanced the intracolonic expression of another chemokine, CCL3, which can exhibit biological effects on leukocytes and non-leukocyte cells, particularly fibroblasts (14, 15). Hence, we investigated the roles of the CCL3 axis in this CAC model and demonstrated that CCL3 and its specific receptor, CCR5, have crucial roles in CAF accumulation in AOM/DSS-induced CAC. Moreover, we provided the first definitive evidence to indicate that leukocyte infiltration is not sufficient, but that the CCL3-CCR5-mediated fibroblast accumulation is additionally required to induce full-blown CAC.

Material and Methods

Mice

Specific pathogen-free seven week-old female Balb/c mice were purchased from Charles River Laboratories (Yokohama, Japan) and were designated as wild-type (WT) mice. CCR5-deficient mice were generated as previously described (16). CCR1-deficient mice (17) were provided by Dr. P. Murphy (NIAID, NIH, Bethesda, MD). CCL3-deficient mice (18) were obtained from the Jackson Laboratory (Bar Harbor, ME). These gene-deficient mice were backcrossed to Balb/c for more than eight generations. All mice were kept under specific pathogen-free conditions with free access to food and water.

AOM/DSS-induced colon carcinogenesis model

Pathogen-free 8- to 12-week old female WT, CCL3-, CCR1-, or CCR5-deficient mice were injected intraperitoneally with 12 mg/kg body weight of AOM dissolved in physiological saline. Five days thereafter, 3.0 % or 4.5 % DSS was given in the drinking water over 5 days, followed by 16 days of regular water and this cycle was repeated a total of 3 times. Body weights were measured every day, and the animals were sacrificed at the indicated time intervals for macroscopical inspection, histological analysis, and total RNA extraction followed by quantitative reverse transcription polymerase chain reaction (qRT-PCR). The detailed procedures of *in vivo* gene transduction are described in Supplementary Methods.

Tumor inoculation

A murine adenocarcinoma cell line, colon 26 (19), was maintained in RPMI with 10% heat-inactivated fetal bovine serum. Sub-confluent cells were collected and resuspended in HBSS. The cell viability was confirmed to be always > 95% by a trypan blue exclusion test. One hundred fifty μl of cell suspensions (50×10^4 cells/head) were injected subcutaneously (s.c.) into the back of WT, CCR1- or CCR5-deficient mice. Tumor sizes were measured every 3 to 4 days using calipers. Tumor volumes were calculated according to an equation of $a \times b^2/2$, where a and b indicate long and short diameters of the tumor, respectively (20).

Fourteen days after tumor cell injection, tumors were removed for immunohistochemical analysis or enzymatically digested using collagenase type I for single cell preparation to conduct a flow cytometry. In another series of experiments, 40 μl of cell suspensions (10 x 10^4 cells/head) were administered to cecum of WT or CCR5-deficient mice. Fourteen days after tumor cell injection, cecum was removed for determination of tumor volume and immunohistochemical analysis.

Isolation of murine fibroblasts from colon tissues

Detailed information on isolation of murine fibroblasts is provided in Supplementary Methods.

Reagents and plasmids

Detailed information on the used reagents and plasmids is provided in Supplementary Methods.

Immunohistochemical analysis and qRT-PCR

Detailed information on immunohistochemical analysis and qRT-PCR is provided in Supplementary Methods.

Statistical analysis

Statistical significance was evaluated using one-way ANOVA, followed by Tukey-Kramer post-hoc test or Dunnet's test. *p* values less than 0.05 were considered statistically significant.

Results

Reduction in AOM/DSS-induced colonic tumorigenesis in CCL3 or CCR5-deficient mice. WT mice given 3.0 % DSS to ingest exhibited a marked body weight loss synchronizing with DSS ingestion (Supplementary Fig. 1). As we previously observed (9, 10), tumors emerged in the colon at 35 days after the initiation of DSS intake, increasing in numbers and size, thereafter, and extending from the middle to distal colon of WT mice at 56 days (Fig. 1A). Given our previous observations indicating the crucial involvement of a macrophage-tropic chemokine, CCL2-mediated macrophage infiltration in this carcinogenesis (10), we investigated the expression of another macrophage-tropic chemokines, CCL3, CCL4, and CCL5, and their receptors, CCR1 and CCR5. *CCL3*, *CCR1*, and *CCR5* mRNA expression levels were augmented in WT mice during the whole course of this carcinogens process, while CCL4 and CCL5 mRNA expression was transiently enhanced but returned to basal level after 35 days when tumor appeared (Fig. 1B). In order to determine the roles of the CCL3 axis, if any, we gave 3.0 % DSS after AOM injection to CCL3-, CCR1-, or CCR5-deficient mice. Three % DSS failed to induce a marked body weight loss (Supplementary Fig. 1) and a large number of tumor formation in CCL3-, CCR1-, or CCR5-deficient mice (Fig. 1A, 1C, and 1D). When the DSS concentration was increased to 4.5 %, all WT mice succumbed to death until 10 days after the first DSS intake, while CCL3-, CCR1- or CCR5-deficient mice exhibited a marked body weight loss synchronizing with DSS ingestion but survived until 56 days (Supplementary Fig. 2). Eventually, CCR1-deficient mice developed a large number of colon tumors, whereas the numbers and size of colon tumors were markedly lower in CCL3- or CCR5-deficient mice (Fig. 1A, 1C, and 1D). However, severe body weight loss would indicate that CCL3-, CCR1- or CCR5-deficient mice developed similar inflammatory reactions when they were given 4.5 % DSS. This assumption was corroborated by the observations that Ly6G-positive granulocytes and F4/80-positive macrophages infiltrated to a similar extent in these three strains when they were given 4.5 % DSS (Fig. 2A). Thus, leukocyte infiltration may be necessary, but not sufficient, to induce full-blown AOM/DSS-induced

CAC in CCL3- or CCR5-deficient mice. Moreover, a double-color immunofluorescence revealed that CCL3 expression was detected on Ly6C-positive cells and α-smooth muscle actin (SMA)-positive cells (Fig. 2B).

Reduced tumor formation correlates with attenuated fibroblast accumulation in the absence of the CCL3 axis. Cancer-associated inflammatory responses consist of fibroblast accumulation as well as leukocyte infiltration (1). In order to prove the roles of fibroblast accumulation in this carcinogenesis model, we evaluated fibrotic changes in this colon carcinogenesis model. In mice given 4.5 % DSS, collagen deposition was increased in CCR1- but not CCL3- or CCR5-deficient mice as revealed by Masson's staining (Fig. 3A). Moreover, larger numbers of intratumoral type I collagen-positive cell numbers were observed in CCR1-deficient mice than CCL3- or CCR5-deficient mice (Fig. 3A and 3B). The intake of 3.0 % DSS after AOM injection did significantly increase type I collagen-positive cells in WT mice on and after 49 days but not at 35 days (Fig. 3C). Thus, fibroblast accumulated after tumors started to appear in colon. On the contrary, type I collagen-positive cell numbers were not increased until 56 days in the mice deficient in *CCL3* or *CCR5* gene (Fig. 3C), as similarly observed when these mice were given 4.5 % DSS (Fig. 3B). Moreover, a double-color immunofluorescence analysis detected CCR5 expression on type I collagen-positive cells (Fig. 3D), consistent with our previous observation on lung fibroblasts at lung metastasis sites (15). We previously proved that CCL3 can induce the migration of fibroblasts in a CCR5-dependent manner (15). We further demonstrated that CCL3 enhanced the *in vitro* proliferation of fibroblasts derived from colon tissues as well as TNF-α (Fig. 3E). These observations would indicate that CCL3-CCR5-mediated fibroblast accumulation is required, in addition to leukocyte infiltration, to induce full-blown colon carcinogenesis, particularly in the later phase.

Reduction in AOM/DSS-induced HB-EGF expression in CCL3- or CCR5-deficient mice. Several lines of evidence indicate that fibroblasts can produce various growth factors including hepatocyte growth factor (HGF), epiregulin (EREG), basic fibroblast

growth factor (bFGF), and HB-EGF to promote tumor progression (21-23). Because fibroblast accumulation was not evident at 35 days, we examined the expression of these factors on and after 35 days. However, we failed to observe differences in HGF, bFGF, and EREG mRNA expression among WT, CCL3-, or CCR5-deficient mice on and after 35 days after DSS injection (Supplementary Fig. 3). On the contrary, HB-EGF mRNA and protein expression was depressed in CCL3- or CCR5-deficient mice, compared with WT mice on and after 49 days (Fig. 4A and 4B), when fibroblast accumulation was evident in WT mice. We further examined mRNA expression of other fibroblast-related molecules such as tenascin C (24), matrix metalloproteinase (MMP)-2 (25), MMP-9 (25), and CXCL1 and CXCL2, mouse functional homologues of IL-8/CXCL8 (26). Among these molecules, only CXCL1 and CXCL2 expression was enhanced during AOM/DSS-induced carcinogenesis and the increases were attenuated in CCL3- or CCR5-deficient mice (Supplementary Fig. 3). A double-color immunofluorescence analysis demonstrated that type I collagen-positive cells expressed HB-EGF (Fig. 4C). Moreover, HB-EGF mRNA was detected selectively in the tumor tissue-derived cell fraction expressing mRNA of type I collagen- and platelet-derived growth factor receptor β chain (PDGFRβ), selective markers of fibroblasts (Figure 4D). Furthermore, CCL3 enhanced HB-EGF expression in colon-derived fibroblasts as well as TNF-α (Fig. 4E), suggesting that CCL3 can sustain HB-EGF expression in fibroblasts accumulated in colon tumor. Finally, we *in vivo* transduced HB-EGF gene into CCL3-deficient mice at 42 days after the initiation of DSS intake. HB-EGF-expression but not control vector transduction increased the tumor numbers (Figure 4F) with few effects on type I collagen-positive cell numbers (Supplementary Fig. 4). These observations suggest that HB-EGF could directly promote tumor formation.

Reduced fibroblast accumulation and tumor formation by CCR5 blockade. In order to address the effects of the CCR5 blockade on tumor progression, we injected colon 26 cells s.c. into WT, CCR1-, or CCR5-deficient mice. Tumor formation was significantly depressed in CCR5-deficient mice, compared with WT or CCR1-deficient mice (Fig. 5A), but with little suppression on the infiltration of F4/80-positive macrophages

and Ly6G-positive granulocytes (Fig. 5B and 5C). On the contrary, type I collagen-positive cell and Ly6C-positive cell numbers were reduced in CCR5-deficient mice, compared with WT or CCR1-deficient mice (Fig. 5D and E). Similarly, tumor formation was significantly depressed in CCR5-deficient mice together with reduced intratumoral type I collagen-positive cell numbers, compared with WT when colon 26 cells were injected into the cecum (Figure 5F and 5G). Finally, we systemically expressed truncated (t)RANTES/CCL5 by using hydrodynamic tail vein injection technique (27, 28) at 56 days after AOM/DSS treatment, when multiple tumors have developed in the colon. Under these conditions, systemic tRANTES/CCL5 expression resulted in sustained expression of this CCR5 antagonist in serum until 70 days after the treatment (Supplementary Fig. 5). Type I collagen-positive cell accumulation, HB-EGF expression, and subsequent tumor formation were significantly reduced, even when the vector was administered after multiple colon tumors have developed (Fig. 6A to 6D). However, tRANTES/CCL5 had few effects on the numbers of Ly6G-positive granulocytes and F4/80-positive macrophages in tumors (Fig. 6E and 6F). These observations further support our conclusion that the CCL3-CCR5 axis could regulate fibroblast accumulation and HB-EGF expression in fibroblasts and that both processes were crucial for tumor progression.

Discussion

CAC can ensue from persistent colonic inflammation consisting of submucosal edema and a massive leukocyte infiltration into the mucosa. Accumulating evidence implicates the crucial roles of infiltration of leukocytes including neutrophils and macrophages in cancer development in AOM/DSS-induced CAC model (9, 10). Similarly, as observed in TNF-Rp55- or CCR2-deficient mice (9, 10), we observed that neutrophil infiltration and subsequent tumor formation was remarkably reduced in CCL3-, CCR1-, or CCR5-deficient mice, which were given 3.0 % DSS solution, compared with WT mice. Of interest is that 4.5 % DSS intake induced a marked infiltration of granulocytes and macrophages in these three strains, to a similar extent as WT mice given 3.0 % DSS. However, only CCR1-deficient mice developed tumors equally as well as WT mice given 3.0 % DSS. These observations would indicate that leukocyte infiltration may be necessary, but not be sufficient to induce full-blown CAC.

Chemokines were originally identified as regulators of leukocyte trafficking, but subsequent studies unraveled their profound effects on other types of cells including endothelial cells and fibroblasts, the cells that contribute, in collaboration with leukocytes, to inflammatory responses including cancer-associated inflammation (29). Moreover, we previously observed that fibroblasts express CCR5 and exhibit chemotaxis in response to CCL3 in a CCR5-dependent manner (15). Hence, we investigated the fibrotic changes in colon after AOM/DSS treatment. We demonstrated that fibroblast accumulation was evident after tumors formed in colon and that it was remarkably reduced in CCL3- or CCR5-deficient mice, compared with WT or CCR1-deficient mice. Likewise, CCR5-deficient mice exhibited reduced tumor growth with attenuated fibroblast accumulation, compared with WT or CCR1-deficient mice when a mouse colon adenocarcinoma cell line was injected s.c. or into cecum. Thus, the CCL3-CCR5-mediated fibroblast accumulation can be additionally required for colon carcinogenesis, particular in its progression phase.

CAFs, fibroblasts present in tumor tissues, can be activated by paracrine signals to produce various growth factors (11). TNF-α is expressed often abundantly in tumor tissues

and can activate CAFs to express various cytokines and chemokines (30). We previously detected TNF-α expression in colon tissues in this model (9). Indeed, TNF-α *in vitro* augmented cell proliferation and HB-EGF expression in colonic fibroblasts equally as well as CCL3. Thus, CCL3, like TNFα, can have profound impacts on fibroblast functions, such as migration, proliferation, and growth factor expression, thereby promoting mainly tumor progression.

CAFs consist of heterogeneous populations with diverse origins; locally resident fibroblasts, cells undergoing epithelial-mesenchymal transition, and bone marrow-derived fibrocytes (11, 31). We previously demonstrated that both fibroblasts and type I collagen-positive CD45-positive fibrocytes exhibited a chemotactic response to CCL3 in a CCR5-dependent manner (14, 15). Although we detected CCR5 expression by fibrocytes as well as fibroblasts in colon tissues, fibrocytes were remarkably less numerous than fibroblasts in colon tissues after AOM/DSS treatment (our unpublished data). Considering that CCL3 can promote fibroblast proliferation, it may be more plausible that the CCL3-CCR5 axis acts mainly on resident fibroblasts in colon tissues.

CAFs produce various growth factors to promote cancer cell growth. Accumulating evidence indicates that fibroblasts are a major source of HGF (32). We also reported HGF production by lung fibroblasts in the mouse lung metastasis model (15), but we could not detect enhanced HGF expression in colon after AOM/DSS treatment, consistent with the previous report (12). CAF-derived epiregulin is proposed to be crucially involved in AOM/DSS-induced neoplasms by activating mitogen-activated protein kinase (MAPK) pathway (13). However, we failed to observe a sustained elevation of epiregulin and the effects of CCL3 or CCR5 deficiency on its expression in colon. On the contrary, HB-EGF expression was markedly attenuated in CCL3- or CCR5-deficient mice, implying that the CCL3-CCR5 axis can regulate HB-EGF expression by fibroblasts in colon. This assumption is further corroborated by the ability of CCL3 to induce HB-EGF expression *in vitro* in fibroblasts.

HB-EGF belongs to epidermal growth factor (EGF) family of growth factors (33). Like other EGF family members, HB-EGF is initially synthesized as a transmembrane

precursor protein and is cleaved at the cell surface by a protease to yield the soluble form by ectodomain shedding (34). The receptors for EGF family members possess tyrosine kinase activity and comprise four members; EGF receptor (EGFR)/ErbB1, ErbB2, ErbB3, and ErbB4 (35). HB-EGF binds predominantly EGFR and ErbB4 to exert its biological effects. EGFR is expressed ubiquitously by various types of epithelial cells although the cellular distribution of ErbB4 still remains to be investigated. Immunohistochemical analyses detected HB-EGF protein in various types of cancer cells including pancreatic (36), hepatocellular (37), colonic (38), gastric (39), and ovarian cancer cells (40). However, in uterine cervical cancer tissues, HG-EGF was expressed primarily in stromal fibroblasts, rather than cancer cells (21), consistent with our observation that HB-EGF was predominantly expressed in type I collagen-positive cells. Thus, fibroblast-derived HB-EGF can act on cancer cells to activate MAPK, P13-Akt, Src and Stat pathways, which exist downstream of its receptors (33, 34), leading to excessive cell growth and invasion, in a paracrine manner. This notion was corroborated by our present observation that *in vivo* HB-EGF gene transduction markedly enhanced tumor formation in CCL3-deficient mice with few effects on fibroblast accumulation at the time, when tumor started to emerge.

Several lines of evidence indicate that HB-EGF can activate NF-κB (41, 42), the transcription factor which is activated most frequently in both inflammatory responses and carcinogenesis (43). Greten and colleagues revealed that NF-κB is activated in both intestinal epithelial cells and infiltrating macrophages in AOM/DSS-induced colon carcinogenesis (44). NF-κB activation in intestinal epithelium mediates anti-apoptotic effects, which can prevent the elimination of premalignant cells (44), in which the β-catenin pathway is activated due to mutations in its gene. Moreover, they demonstrated that chronic epithelial NF-κB activation can enhance inducible NO synthase-mediated DNA damage to accelerate *APC* loss (45). Thus, in addition to its direct mitogenic effects on epithelial cells, HB-EGF can promote colon carcinogenesis by activating NF-κB.

We utilized the in vivo gene transduction of tRANTES/CCL5, which can antagonize the interaction between CCR5 and CCR5-binding chemokines, CCL3, CCL4, and CCL5 (46), in order to block CCR5-mediated signals in this model. It is interesting that

tRANTES/CCL5 gene transduction reduced the tumor numbers even when it was administered after multiple tumors already developed. These observations would indicate that colon cancer, particularly CAC, can be treated with a CCR5 antagonist with a small molecular weight, which has been used for the treatment of AIDS patients and is well tolerated (47, 48). Moreover, tRANTES/CCL5 simultaneously attenuated fibroblast accumulation and HB-EGF expression, with few effects on the infiltration of granulocytes and macrophages, the cells which are presumed to have crucial roles in this colon carcinogenesis (9, 10). Thus, the selective blockade of fibroblast trafficking and/or functions may be effective in counteracting the progression of cancer characterized by the presence of abundant CAFs.

Acknowledgement

We thank Dr. Yasuhiko Kitadai (Hiroshima University) for his invaluable advice on experimental procedures. We would like to express our sincere gratitude to Dr. Joost J. Oppenheim (NCI-Frederick, Frederick, MD) for his critical review of the manuscript.

References

1. Dvorak HF. Tumors: wounds that do not heal. Similarities between tumor stroma generation and wound healing. *N Engl J Med.* 1986;**315**:1650-9.
2. Balkwill F, Mantovani A. Inflammation and cancer: back to Virchow? *Lancet* 2001;**357**:539-45.
3. Fiocchi C. Inflammatory bowel disease: etiology and pathogenesis. *Gastroenterology* 1998;**115**:182-205.
4. Brentnall TA, Crispin DA, Bronner MP, Cherian SP, Hueffed M, Rabinovitch PS, Rubin CE, Haggitt RC, Boland CR. Microsatellite instability in nonneoplastic mucosa from patients with chronic ulcerative colitis. *Cancer Res.* 1996;**56**:1237-40.
5. Okayasu I, Hatakeyama S, Yamada M, Ohkusa T, Inagaki Y, Nakaya R. A novel method in the induction of reliable experimental acute and chronic ulcerative colitis in mice. *Gastroenterology* 1990;**98**:694-702.
6. Okayasu I, Yamada M, Mikami T, Yoshida T, Kanno J, Ohkusa T. Dysplasia and carcinoma development in a repeated dextran sulfate sodium-induced colitis model. *J gastroenterol hepatol.* 2002;**17**:1078-83.
7. Okayasu I, Ohkusa T, Kajiura K, Kanno J, Sakamoto S. Promotion of colorectal neoplasia in experimental murine ulcerative colitis. *Gut* 1996;**39**:87-92.
8. Takahashi M, Wakabayashi K. Gene mutations and altered gene expression in azoxymethane-induced colon carcinogenesis in rodents. *Cancer Sci.* 2004;**95**:475-80.
9. Popivanova BK, Kitamura K, Wu Y, Kondo T, Kagaya T, Kaneko S, Oshima M, Fujii C, Mukaida N. Blocking TNF-alpha in mice reduces colorectal carcinogenesis associated with chronic colitis. *J Clin Invest.* 2008;**118**:560-70.
10. Popivanova BK, Kostadinova FI, Furuichi K, Shamekh MM, Kondo T, Wada T, Egashira K, Mukaida N. Blockade of a chemokine, CCL2, reduces chronic colitis-associated carcinogenesis in mice. *Cancer Res.* 2009;**69**:7884-92.
11. Servais C, Erez N. From sentinel cells to inflammatory culprits: cancer-associated fibroblasts in tumour-related inflammation. *J Pathol.* 2013;**229**:198-207.

12. Koliaraki V, Roulis M, Kollias G. Tpl2 regulates intestinal myofibroblast HGF release to suppress colitis-associated tumorigenesis. *J Clin Invest.* 2012;**122**:4231-42.
13. Neufert C, Becker C, Tureci O, Waldner MJ, Backert I, Floh K, Atreya I, Leppkes M, Jefremow A, Vieth M, Schneider-Stock R, Klinger P, et al. Tumor fibroblast-derived epiregulin promotes growth of colitis-associated neoplasms through ERK. *J Clin Invest.* 2013;**123**:1428-43.
14. Ishida Y, Kimura A, Kondo T, Hayashi T, Ueno M, Takakura N, Matsushima K, Mukaida N. Essential roles of the CC chemokine ligand 3-CC chemokine receptor 5 axis in bleomycin-induced pulmonary fibrosis through regulation of macrophage and fibrocyte infiltration. *Am J Pathol.* 2007;**170**:843-54.
15. Wu Y, Li YY, Matsushima K, Baba T, Mukaida N. CCL3-CCR5 axis regulates intratumoral accumulation of leukocytes and fibroblasts and promotes angiogenesis in murine lung metastasis process. *J Immunol.* 2008;**181**:6384-93.
16. Murai M, Yoneyama H, Ezaki T, Suematsu M, Terashima Y, Harada A, Hamada H, Asakura H, Ishikawa H, Matsushima K. Peyer's patch is the essential site in initiating murine acute and lethal graft-versus-host reaction. *Nat. Immunol.* 2003;**4**:154-60.
17. Gao JL, Wynn TA, Chang Y, Lee EJ, Broxmeyer HE, Cooper S, Tiffany HL, Westphal H, Kwon-Chung J, Murphy PM. Impaired host defense, hematopoiesis, granulomatous inflammation and type 1-type 2 cytokine balance in mice lacking CC chemokine receptor 1. *J Exp Med.* 1997;**185**:1959-68.
18. Cook DN, Beck MA, Coffman TM, Kirby SL, Sheridan JF, Pragnell IB, Smithies O. Requirement of MIP-1 alpha for an inflammatory response to viral infection. *Science* 1995;**269**:1583-5.
19. Corbett TH, Griswold DP, Jr., Roberts BJ, Peckham JC, Schabel FM, Jr. Tumor induction relationships in development of transplantable cancers of the colon in mice for chemotherapy assays, with a note on carcinogen structure. *Cancer Res.* 1975;**35**:2434-9.
20. Kitakata H, Nemoto-Sasaki Y, Takahashi Y, Kondo T, Mai M, Mukaida N. Essential roles of tumor necrosis factor receptor p55 in liver metastasis of intrasplenic administration of colon 26 cells. *Cancer Res.* 2002;**62**:6682-7.

21. Murata T, Mizushima H, Chinen I, Moribe H, Yagi S, Hoffman RM, Kimura T, Yoshino K, Ueda Y, Enomoto T, Mekada E. HB-EGF and PDGF mediate reciprocal interactions of carcinoma cells with cancer-associated fibroblasts to support progression of uterine cervical cancers. *Cancer Res.* 2011;**71**:6633-42.

22. Jain RK, Lahdenranta J, Fukumura D. Targeting PDGF signaling in carcinoma-associated fibroblasts controls cervical cancer in mouse model. *PLoS Med.* 2008;**5**:e24.

23. Li Q, Wang W, Yamada T, Matsumoto K, Sakai K, Bando Y, Uehara H, Nishioka Y, Sone S, Iwakiri S, Itoi K, Utsugi T, et al. Pleural mesothelioma instigates tumor-associated fibroblasts to promote progression via a malignant cytokine network. *Am J Pathol.* 2011;**179**:1483-93.

24. Allen M, Louise Jones J. Jekyll and Hyde: the role of the microenvironment on the progression of cancer. *J Pathol.* 2011;**223**:162-76,

25. Noël A, Jost M, Maquoi E. Matrix metalloproteinases at cancer tumor-host interface. *Semin Cell Dev Biol.* 2008;**19**:52-60.

26. Harada A, Sekido N, Akahoshi T, Wada T, Mukaida N, Matsushima K.. Essential involvement of interleukin-8 (IL-8) in acute inflammation. *J Leukoc Biol.* 1994;**56**:559-64.

27. Zhang G, Vargo D, Budker V, Armstrong N, Knechtle S, Wolff JA. Expression of naked plasmid DNA injected into the afferent and efferent vessels of rodent and dog livers. *Hum Gene Ther.* 1997;**8**:1763-72.

28. Zhang G, Budker V, Wolff JA. High levels of foreign gene expression in hepatocytes after tail vein injections of naked plasmid DNA. *Hum Gene Ther.* 1999;**10**:1735-7.

29. Mukaida N, Baba T. Chemokines in tumor development and progression. *Exp Cell Res.* 2012;**318**:95-102.

30. Mueller L, Goumas FA, Affeldt M, Sandtner S, Gehling UM, Brilloff S, Walter J, Karnatz N, Lamszus K, Rogiers X, Broering DC. Stromal fibroblasts in colorectal liver metastases originate from resident fibroblasts and generate an inflammatory microenvironment. *Am J Pathol.* 2007;**171**:1608-18.

31. Mishra P, Banerjee D, Ben-Baruch A. Chemokines at the crossroads of tumor-fibroblast interactions that promote malignancy. *J Leukoc Biol.* 2011;**89**:31-9.

32. Matsumoto K, Nakamura T. Hepatocyte growth factor and the Met system as a mediator of tumor-stromal interactions. *Int J Cancer.* 2006;**119**:477-83.

33. Miyamoto S, Yagi H, Yotsumoto F, Kawarabayashi T, Mekada E. Heparin-binding epidermal growth factor-like growth factor as a novel targeting molecule for cancer therapy. *Cancer Sci.* 2006;**97**:341-7.

34. Raab G, Klagsbrun M. Heparin-binding EGF-like growth factor. *Biochim Biophys Acta.* 1997;**1333**:F179-99.

35. Hynes NE, Lane HA. ERBB receptors and cancer: the complexity of targeted inhibitors. *Nat Rev Cancer* 2005;**5**:341-54.

36. Ito Y, Higashiyama S, Takeda T, Yamamoto Y, Wakasa KI, Matsuura N. Expression of heparin-binding epidermal growth factor-like growth factor in pancreatic adenocarcinoma. *Int J Pancreatol.* 2001;**29**:47-52.

37. Ito Y, Takeda T, Higashiyama S, Sakon M, Wakasa KI, Tsujimoto M, Monden M, Matsuura N. Expression of heparin binding epidermal growth factor-like growth factor in hepatocellular carcinoma: an immunohistochemical study. *Oncol Rep.* 2001;**8**:903-7.

38. Ito Y, Higashiyama S, Takeda T, Okada M, Matsuura N. Bimodal expression of heparin-binding EGF-like growth factor in colonic neoplasms. *Anticancer Res.* 2001;**21**:1391-4.

39. Murayama Y, Miyagawa J, Shinomura Y, Kanayama S, Isozaki K, Yamamori K, Mizuno H, Ishiguro S, Kiyohara T, Miyazaki Y, Taniguchi N, Higashiyama S, et al. Significance of the association between heparin-binding epidermal growth factor-like growth factor and CD9 in human gastric cancer. *Int J Cancer.* 2002;**98**:505-13.

40. Miyamoto S, Hirata M, Yamazaki A, Kageyama T, Hasuwa H, Mizushima H, Tanaka Y, Yagi H, Sonoda K, Kai M, Kanoh H, Nakano H, et al. Heparin-binding EGF-like growth factor is a promising target for ovarian cancer therapy. *Cancer Res.* 2004;**64**:5720-7.

41. Lee KS, Park JH, Lee S, Lim HJ, Choi HE, Park HY. HB-EGF induces delayed STAT3 activation via NF-kappaB mediated IL-6 secretion in vascular smooth muscle cell.

Biochim Biophys Acta. 2007;**1773**:1637-44.

42. Rahman FB, Kadowaki Y, Ishihara S, Tobita H, Imaoka H, Fukuhara H, Aziz MM, Furuta K, Amano Y, Kinoshita Y. Fibroblast-derived HB-EGF promotes Cdx2 expression in esophageal squamous cells. *Lab Invest.* 2010;**90**:1033-48.
43. Naugler WE, Karin M. NF-kappaB and cancer-identifying targets and mechanisms. *Curr Opin Genet Dev.* 2008;**18**:19-26.
44. Greten FR, Eckmann L, Greten TF, Park JM, Li ZW, Egan LJ, Kagnoff MF, Karin M. IKKbeta links inflammation and tumorigenesis in a mouse model of colitis-associated cancer. *Cell* 2004;**118**:285-96.
45. Shaked H, Hofseth LJ, Chumanevich A, Chumanevich AA, Wang J, Wang Y, Taniguchi K, Guma M, Shenouda S, Clevers H, Harris CC, Karin M. Chronic epithelial NF-kappaB activation accelerates APC loss and intestinal tumor initiation through iNOS up-regulation. *Proc Natl Acad Sci U S A.* 2012;**109**:14007-12.
46. Ylisastigui L, Vizzavona J, Drakopoulou E, Paindavoine P, Calvo CF, Parmentier M, Gluckman JC, Vita C, Benjouad A. Synthetic full-length and truncated RANTES inhibit HIV-1 infection of primary macrophages. *AIDS.* 1998;**12**:977-84.
47. Westby M, van der Ryst E. CCR5 antagonists: host-targeted antivirals for the treatment of HIV infection. *Antivir Chem Chemother.* 2005;**16**:339-54.
48. Chen W, Zhan P, De Clercq E, Liu X. Recent progress in small molecule CCR5 antagonists as potential HIV-1 entry inhibitors. *Curr Pharm Des.* 2012;**18**:100-12.

Legends to Figures

Figure 1 The involvement of the CCL3-CCR5 axis in AOM/DSS-induced colon carcinogenesis. **A.** Macroscopic and microscopic appearances of colon of WT, CCL3-, CCR1-, and CCR5-deficient mice after AOM/DSS treatment. Colons were removed from WT mice at 56 days after the mice were given either 3.0 % or 4.5 % DSS in combination with AOM pretreatment. Macroscopic appearances of colon tissues are shown in the upper panels, while HE-stained colon tissues are shown in the lower panels. Insets indicate enlarged area of tumor sites. Scale bars represent 100 μm. Representative results from 10 independent animals are shown here. **B.** *CCL3*, *CCL4*, *CCL5*, *CCR1* and *CCR5* gene expression in the colons of WT mice. The levels of mRNA were quantified by qRT-PCR from the colon obtained at the indicated time intervals and normalized to the level of HPRT mRNA. Data represent the mean + SEM (n=5 animals). *, $p<0.05$; **, $p<0.01$ vs. untreated. **C.** Tumor numbers after AOM/DSS treatment. Colons were removed at 56 days after the mice were given either 3.0 % or 4.5 % DSS in combination with AOM pretreatment, to determine the numbers of macroscopic tumors. Data represent the mean + SEM (n=5 animals). **, $p<0.01$; n.s., not significant. **D.** Tumor size after AOM/DSS treatment. Colons were removed at 56 days after the mice were given 3.0 % or 4.5 % DSS in combination with AOM pretreatment, to determine the size of macroscopic tumors. Each symbol represents the size of tumors. The bars represent the average of each group. *, $p<0.05$; n.s., not significant.

Figure 2 Inflammatory cell infiltration and CCL3-expressing cells after AOM/DSS treatment. **A.** Colons were removed at 49 days after the mice were given either 3.0 % or 4.5 % DSS combined with AOM pretreatment. The obtained tissues were fixed and immunostained with either anti-Ly6G or anti-F4/80 antibodies to determine the numbers of Ly6G-positive granulocytes (left panel) or F4/80-positive macrophages (right panel), respectively. All values represent the mean + SEM (n=10 animals). *, $p<0.05$, n.s., not significant. **B.** Immunofluorescence detection of CCL3-expressing cells. Colons were

obtained from WT mice at 49 days after the initiation of DSS treatment. Double-color immunofluorescence analysis was conducted with the combination of anti-CCL3 and anti-F4/80 (top row), that of anti-CCL3 and anti-Ly6C (middle row), or that of anti-CCL3 and anti-αSMA (bottom row). Representative results from 5 independent experiments are shown here. Scale bars represent 100 μm.

Figure 3 The effects of the CCL3-CCR5 axis on fibroblasts. **A.** Colons were removed at 56 days after the mice were given 4.5 % DSS combined with AOM pretreatment. The obtained tissues were fixed, and immunostained with anti-type I collagen antibodies (upper panels) or were stained with Masson's trichrome solution (lower panels). Representative results from 5 mice are shown here. Scale bars represent 100 μm. **B.** Type I collagen-positive areas were determined inside tumor tissues of colon obtained at 56 days after the mice were given 4.5 % DSS combined with AOM pretreatment. All values represent the mean + SEM (n=5 animals). *, $p<0.05$, **, $p<0.01$. **C.** Type I collagen-positive areas were determined inside colon tumor tissues or the corresponding colon tissues obtained at the indicated time intervals after the mice were given 3.0 % DSS combined with AOM pretreatment. All values represent the mean + SEM (n=5 animals). *, $p<0.05$, **, $p<0.01$, n.s., not significant. **D.** Immunofluorescence detection of CCR5-expressing cells. Colons were obtained from WT mice at 56 days after the initiation of DSS treatment. Double-color immunofluorescence analysis was conducted with the combination of anti-CCR5 and anti-F4/80 (top row) or that of anti-CCR5 and anti-type I collagen antibodies (bottom row). Representative results from 5 independent experiments are shown here. Scale bars represent 100 μm. **E.** CCL3-induced fibroblast proliferation. Fibroblasts were incubated in the presence of CCL3 (100 ng/ml) or TNF-α (1 ng/ml) for 2 days. The results are shown with the ratio compared to medium-treated sample. All values represent the mean + SD (n=5). *, $p<0.05$.

Figure 4. HB-EGF expression and its role in carcinogenesis. **A.** The levels of *HB-EGF* mRNA were quantified by qRT-PCR on total RNAs extracted from the colon of WT, CCL3-,

or CCR5-deficient mice and normalized to the level of HPRT mRNA. All values represent the mean + SD (n=5 animals). *, $p<0.05$, WT vs. CCL3- or CCR5-deficient mice. **B.** HB-EGF protein expression in the colons of mice. Colon tissues were obtained from WT, CCL3-deficient, and CCR5-deficient mice and the levels of HB-EGF protein in the colon extracts were quantified by using ELISA. All values represent the mean + SD (n=3 animals). *, $p<0.05$, WT vs. CCL3- or CCR5-deficient mice. **C.** Double-color immunofluorescence analysis was conducted with the combination of anti-type I collagen and anti-HB-EGF antibodies. Signals were digitally merged. Representative results from 5 independent experiments are shown here. Scale bars represent 100 μm. **D.** Total RNAs were extracted from the colon tumor tissues obtained from CD31- and CD45-positive fibroblast-enriched fraction and unseparated cell fraction to determine *HB-EGF*, *type I collagen*, *PDGFRβ* mRNA expression by qRT-PCR and normalized to the level of HPRT mRNA. All values represent the mean + SD (n=5). *, $p<0.05$. **E.** CCL3-induced HB-EGF expression in fibroblasts. Fibroblasts were obtained from colon as described in Supplementary Methods and were incubated in the presence of CCL3 (100 ng/ml) or TNF-α (1 ng/ml) for 2 days. HB-EGF mRNA was quantified by qRT-PCR and normalized to the level of GAPDH mRNA. All values represent the mean + SEM (n=5). *, $p<0.05$. **F.** HB-EGF pLIVE vector was *in vivo* transduced to CCL3-deficient mice at 42 days after the initiation of DSS intake. At 56 days after the initiation of DSS intake, colons were removed to determine the numbers of macroscopic tumors. All values represent the mean + SD (n=5 animals). *, $p<0.05$.

Figure 5. Reduced tumor formation in CCR5-deficient mice after injection of colon 26 cells. **A.** to **E**. A mouse colon adenocarcinoma cell line, colon 26, were injected s.c. into WT, CCR1-deficient, or CCR5-deficient mice. **A.** Tumor volumes were determined at the indicated time intervals. All values represent the mean ± SD (n=5 animals). *, $p<0.05$; **, $p<0.01$. **B.** to **D.** Tumor tissues were obtained at 14 days after the tumor inoculation, to determine the numbers of intratumoral F4/80-positive macrophages (**B**) or Ly6G-positive granulocytes (**C**) and type I collagen-positive areas (**D**). All values represent the mean + SD

(n=5 animals). *, $p<0.05$, **, $p<0.01$, n.s., not significant. **E.** Single cell populations were obtained from tumor tissues and were subjected to a flow cytometric analysis to determine Ly6C-positive cell numbers. All values represent the mean + SD (n=5 animals). *, $p<0.05$. **F.** and **G.** Reduced tumor formation and fibroblast accumulation in CCR5-deficient mice after orthotopic injection of colon 26 cells into cecum. **F.** Cecum was obtained at 14 days after the injection to determine the tumor volumes macroscopically. Each symbol represents the size of tumors. **G.** Type I collagen-positive areas inside tumor tissues were determined on the cecum obtained at 14 days after the injection. All values represent the mean + SD (n>5 animals). *, $p<0.05$.

Figure 6. Reduced tumor formation by CCR5 blockade. WT mice were treated with 3.0 % DSS in combination with AOM pretreatment. At 56 days after the initiation of DSS intake, the mice were administered with either tRANTES/CCL5 expression or control vector. **A.** Animals were sacrificed to obtain colon at each time point until 77 days after the initiation of DSS intake, to determine tumor numbers macroscopically. All values represent the mean + SD (n=5 animals) *, $p<0.05$. **B.** to **F.** Twenty-one days after either tRANTES/CCL5 expression or control vector administration (77 days after the initiation of DSS intake), colon was removed to determine type I collagen-positive areas (**B**), HB-EGF mRNA expression normalized to the level of HPRT (**C**), HB-EGF protein levels (**D**), Ly6G-positive granulocyte numbers (**E**), F4/80-positive macrophage numbers (**F**). All values represent the mean + SD (n=5 animals). *, $p<0.05$; n.s., not significant.

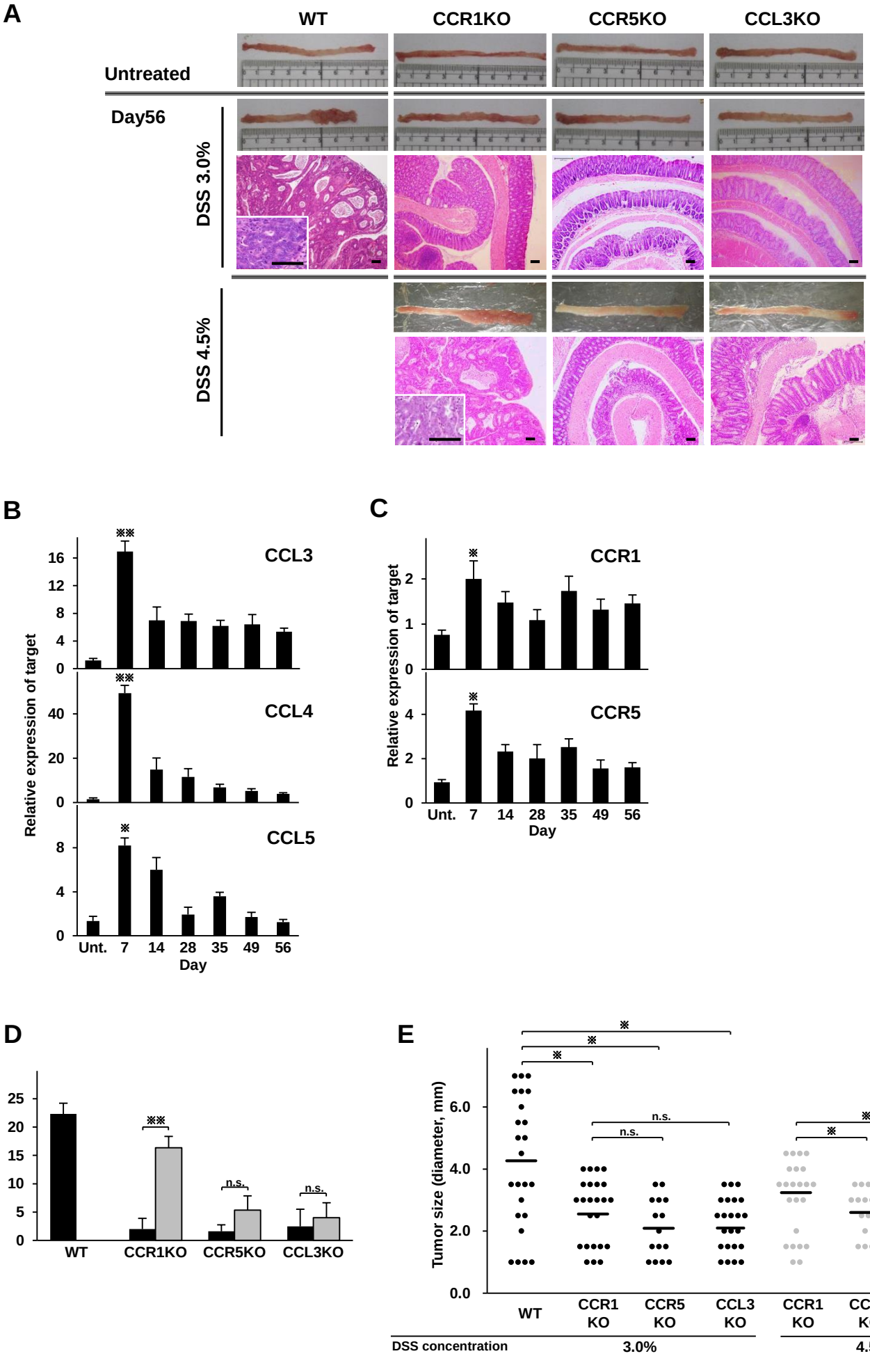
A
WT
CCR1KO
CCR5KO
CCL3KO
Untreated
Day56
DSS 3.0%
DSS 4.5%
B
CCL3
CCL4
CCL5
Relative expression of target
Unt. 7 14 28 35 49 56
Day
C
CCR1
CCR5
Relative expression of target
Unt. 7 14 28 35 49 56
Day
D
Tumor numbers
WT
CCR1KO
CCR5KO
CCL3KO
n.s.
E
Tumor size (diameter, mm)
n.s.
WT
CCR1 KO
CCR5 KO
CCL3 KO
DSS concentration
3.0%
4.5%

A

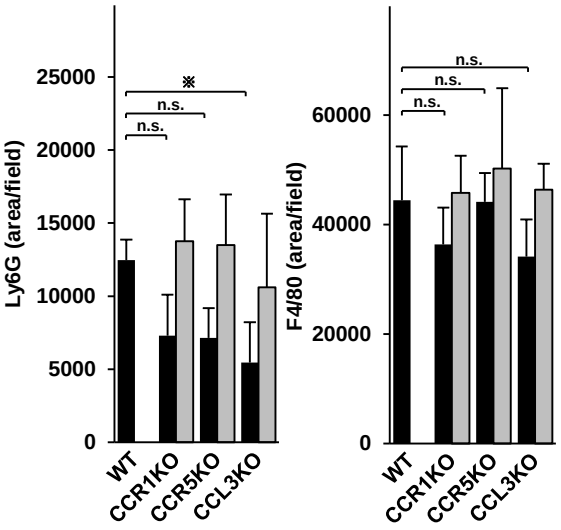
Ly6G (area/field)
25000
20000
15000
10000
5000
0
※
n.s.
n.s.
WT
CCR1KO
CCR5KO
CCL3KO
F4/80 (area/field)
60000
40000
20000
0
n.s.
n.s.
n.s.
WT
CCR1KO
CCR5KO
CCL3KO

B

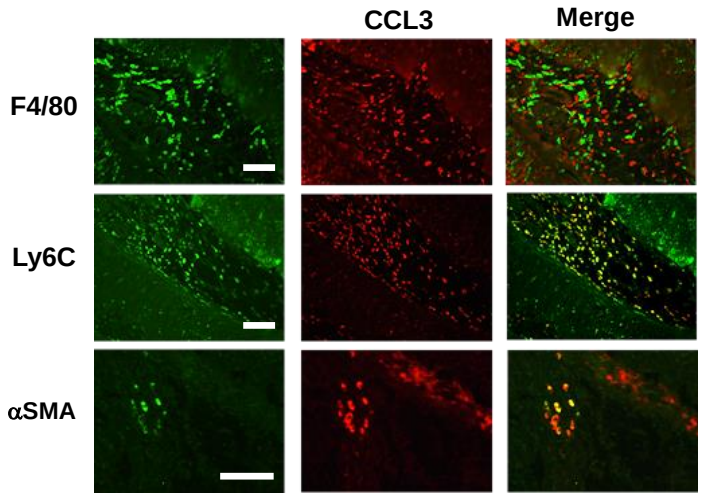
CCL3
Merge
F4/80
Ly6C
αSMA

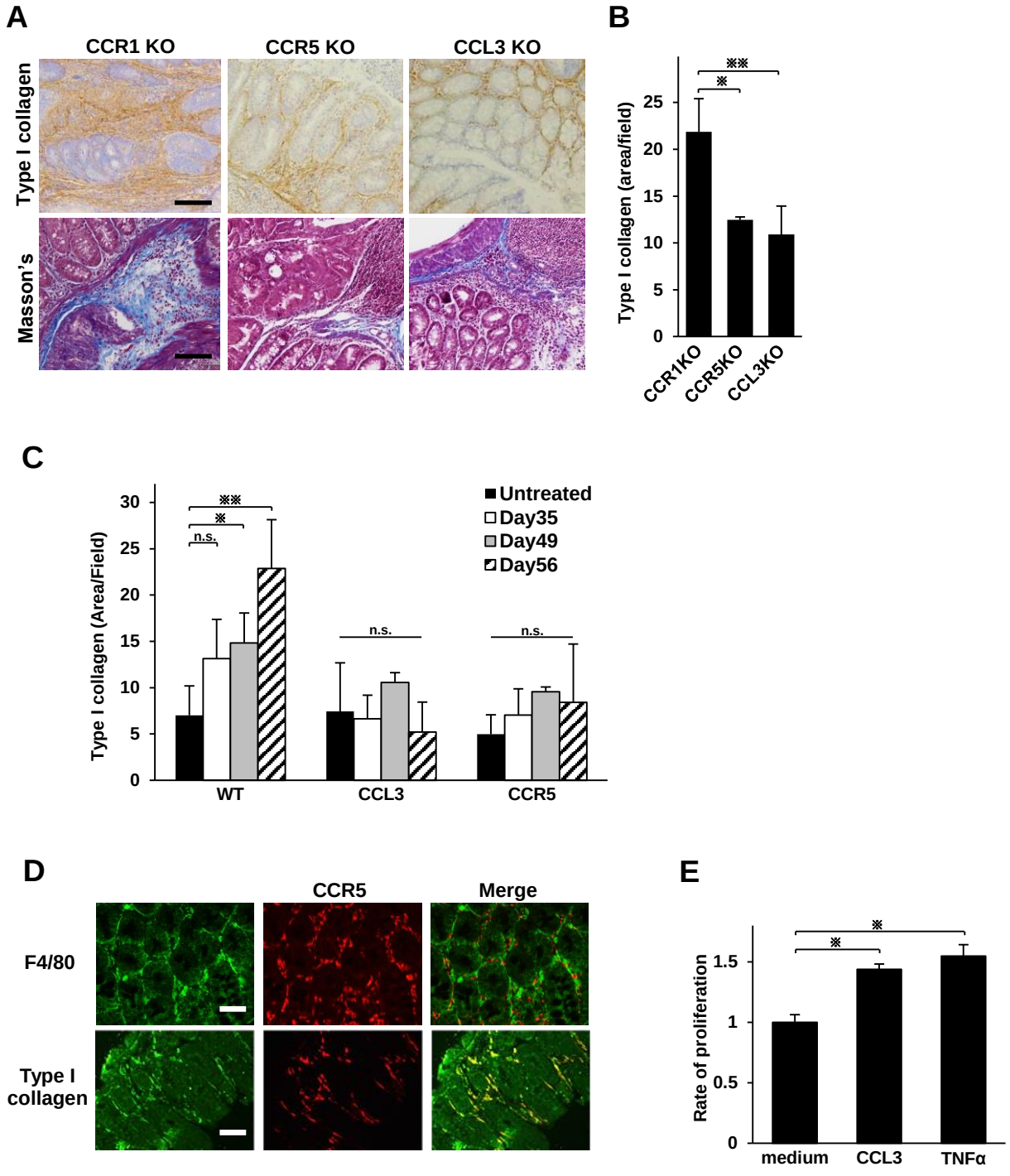
A
CCR1 KO
CCR5 KO
CCL3 KO
Type I collagen
Masson's
B
Type I collagen (area/field)
※※
※
CCR1KO
CCR5KO
CCL3KO
C
Type I collagen (Area/Field)
Untreated
Day35
Day49
Day56
n.s.
WT
CCL3
CCR5
D
CCR5
Merge
F4/80
Type I collagen
E
Rate of proliferation
medium
CCL3
TNFα

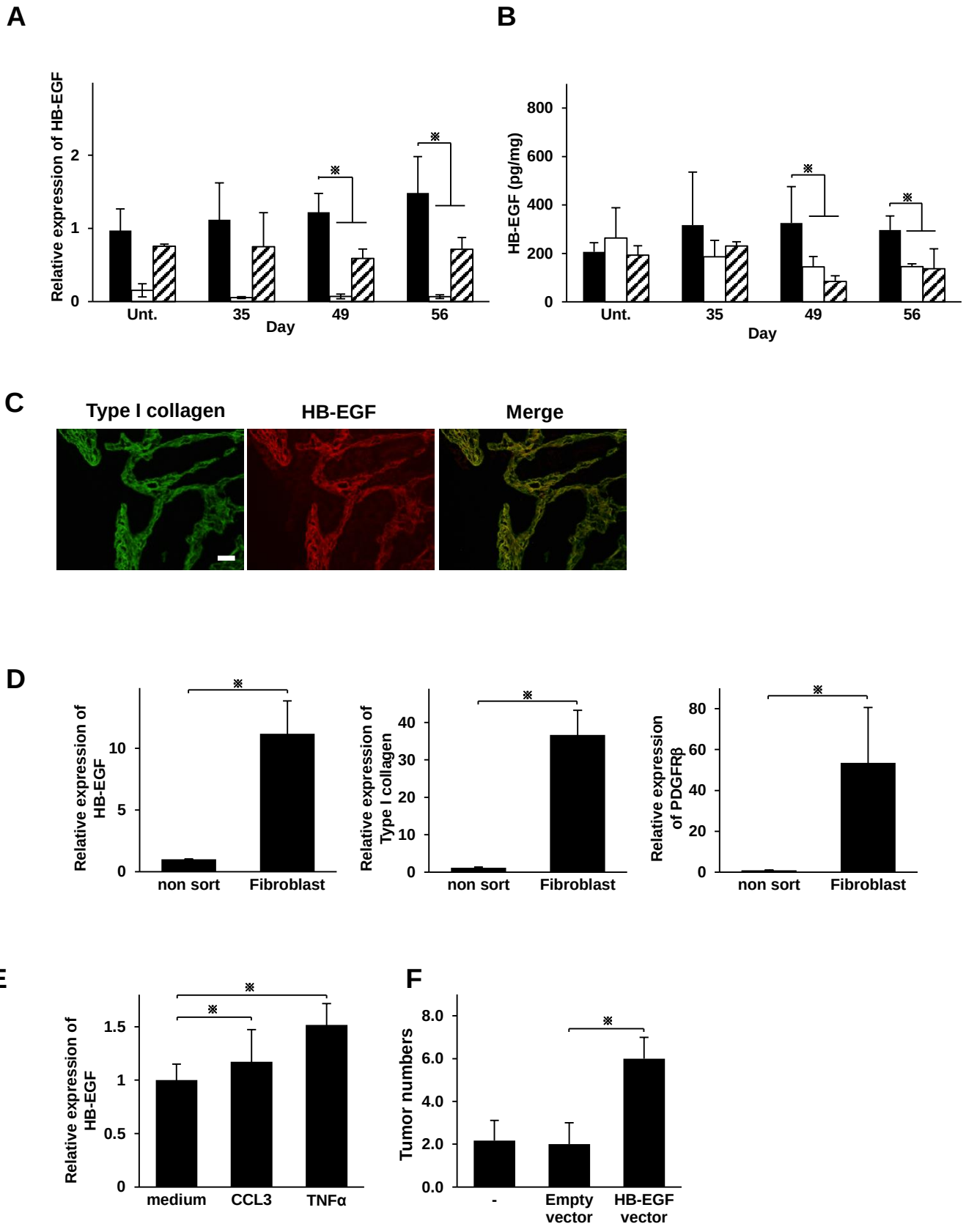
A
Relative expression of HB-EGF
0
1
2
Unt.
35
49
56
Day
※
B
HB-EGF (pg/mg)
0
200
400
600
800
Unt.
35
49
56
Day
※
C
Type I collagen
HB-EGF
Merge
D
Relative expression of HB-EGF
0
5
10
non sort
Fibroblast
※
Relative expression of Type I collagen
0
10
20
30
40
non sort
Fibroblast
※
Relative expression of PDGFRβ
0
20
40
60
80
non sort
Fibroblast
※
E
Relative expression of HB-EGF
0
0.5
1
1.5
medium
CCL3
TNFα
※
※
F
Tumor numbers
0.0
2.0
4.0
6.0
8.0
-
Empty vector
HB-EGF vector
※

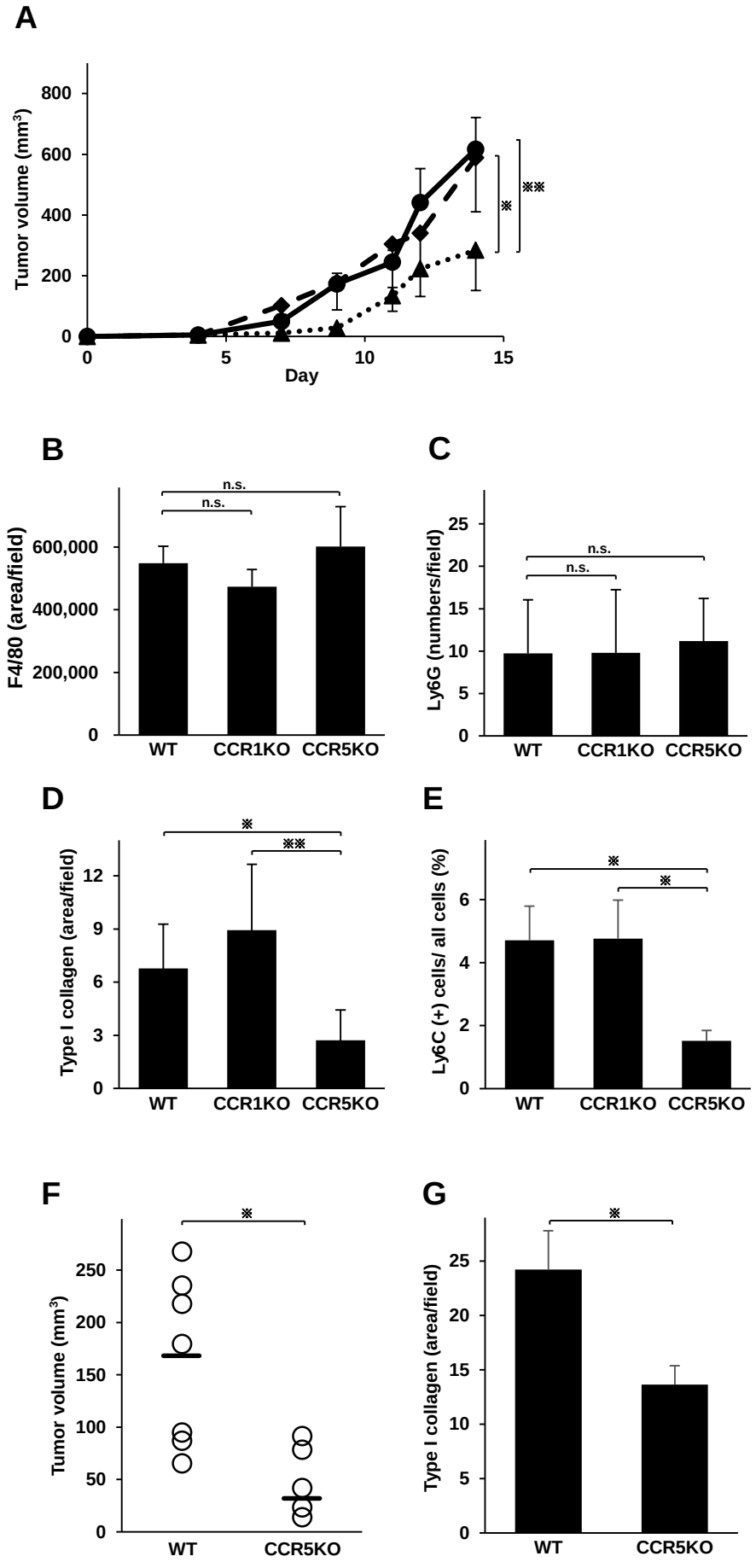
A
Tumor volume (mm3)
800
600
400
200
0
0
5
10
15
Day
※
※※
B
F4/80 (area/field)
600,000
400,000
200,000
0
n.s.
n.s.
WT
CCR1KO
CCR5KO
C
Ly6G (numbers/field)
25
20
15
10
5
0
n.s.
n.s.
WT
CCR1KO
CCR5KO
D
Type I collagen (area/field)
12
9
6
3
0
※
※※
WT
CCR1KO
CCR5KO
E
Ly6C (+) cells/ all cells (%)
6
4
2
0
※
※
WT
CCR1KO
CCR5KO
F
Tumor volume (mm3)
250
200
150
100
50
0
※
WT
CCR5KO
G
Type I collagen (area/field)
25
20
15
10
5
0
※
WT
CCR5KO

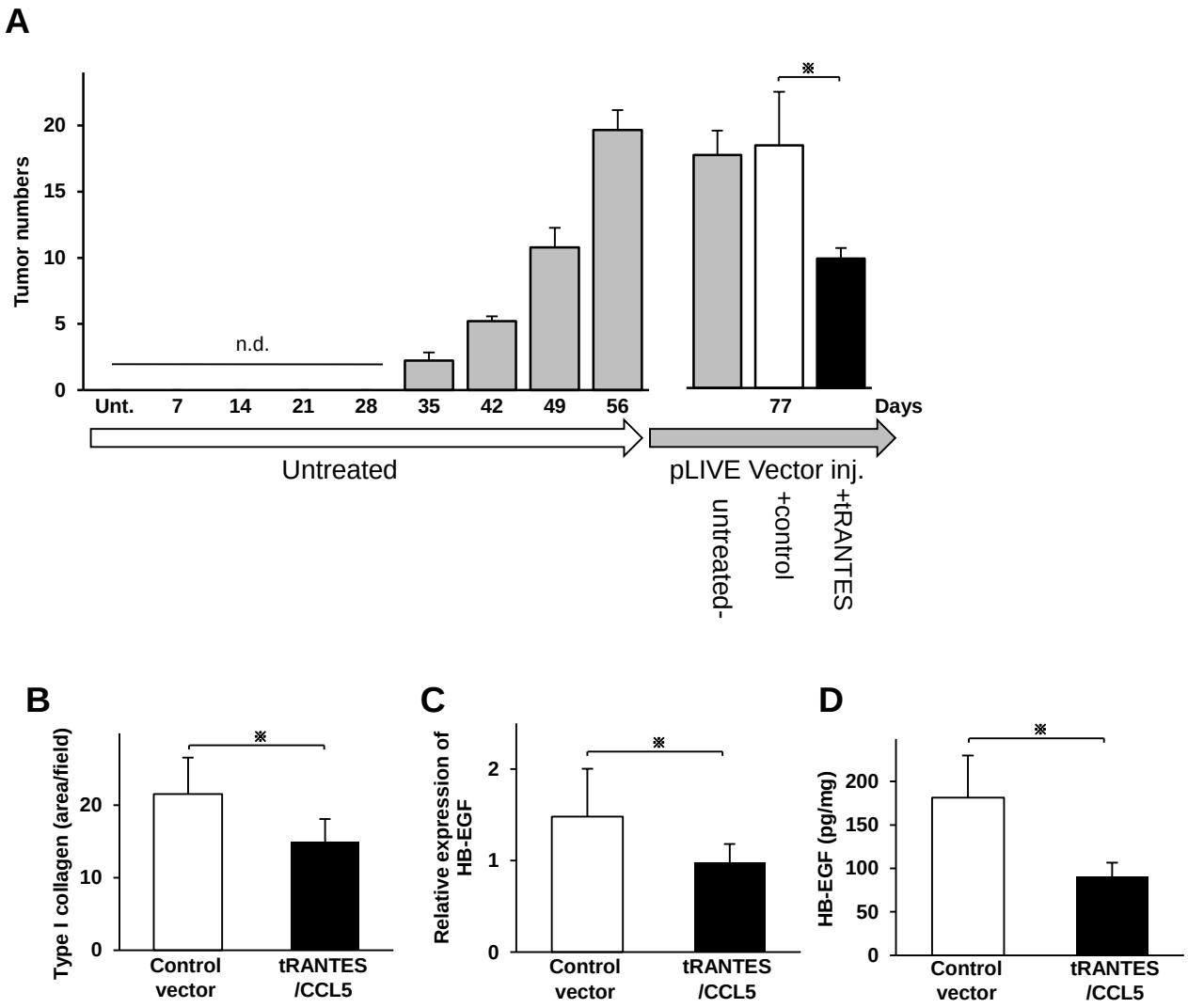
A
Tumor numbers
20
15
10
5
0
n.d.
※
Unt.
7
14
21
28
35
42
49
56
77
Days
Untreated
pLIVE Vector inj.
untreated-
+control
+tRANTES
B
Type I collagen (area/field)
20
10
0
※
Control vector
tRANTES /CCL5
C
Relative expression of HB-EGF
2
1
0
※
Control vector
tRANTES /CCL5
D
HB-EGF (pg/mg)
200
150
100
50
0
※
Control vector
tRANTES /CCL5

Crucial Involvement of the CCL3-CCR5 Axis-mediated Fibroblast Accumulation in Colitis-associated Carcinogenesis in Mice

Soichiro Sasaki,[1,2] Tomohisa Baba,[1] Kei Shinagawa,[3] Kouji Matsushima,[2,4] and Naofumi Mukaida[1,2]

[1]Division of Molecular Bioregulation, Cancer Research Institute, Kanazawa University, Kanazawa, Japan; [2]Japan Science and Technology Agency, Core Research for Evolutionary Science and Technology, Tokyo, Japan; [3]Department of Gastroenterology and Metabolism, Graduate School of Biomedical Sciences, Hiroshima University, Hiroshima, Japan; [4]Department of Molecular Preventive Medicine, Graduate School of Medicine, University of Tokyo, Tokyo, Japan

Supplementary Methods

Reagents and antibodies

AOM and DSS (MW 36,000–50,000) were purchased from Sigma-Aldrich (St. Louis) and MP Biochemicals Inc. (Auroa), respectively. Mouse CCL3 and TNF-α were obtained from Peprotech Inc. (Rocky Hill). The following antibodies were used as the primary antibodies for immunohistochemical or immunofluorescence analyses: goat anti-mouse CCL3 antibody (R&D Systems); goat anti-mouse CCR5 antibody (Santa Cruz Biotechnology); mouse anti-mouse α smooth muscle actin (αSMA) antibody (DAKO); rat anti-mouse Ly6C antibody (Abcam); rat anti-mouse F4/80 antibody (Serotec); rat anti-mouse Ly6G antibody (BD Biosciences); rabbit anti-HB-EGF antibody (Bioss); rabbit anti-type I collagen antibody (Abcam). FITC-rat anti-Ly6C antibody (BD Biosciences) was used for the flow cytometric analysis.

Plasmids

Mouse CCL5 (RANTES) cDNA, which lacks amino-terminal 8 residues, and mouse heparin-binding epidermal growth factor-like growth factor (HB-EGF) cDNA were cloned by reverse transcriptase (RT)-PCR using mouse lung tissue-derived mRNA as a template. The resultant cDNA was inserted into pLIVE-vector (Mirus Corporation) to generate the truncated (t)RANTES/CCL5-pLIVE vector that can express tRANTES/CCL5 protein linked with a Flag tag in its carboxyl-terminal portion or HB-EGF-pLIVE vector. pLIVE-vector without any insert was used as a control plasmid. All the plasmids were isolated by using a Plasmid DNA Purification kit (MACHEREY-NAGEL GmbH).

In vivo transduced gene mouse mode

In some experiments, at 56 days after the initiation of the first DSS intake, WT mice were injected with either tRANTES/CCL5-pLIVE or control vector at a dose of 10 μg/head by

using TransIT-EE Hydrodynamic Delivery Solution (Mirus Corporation) according to the manufacturer's instructions (1, 2). In another series of experiments, at 42 days after the initiation of the first DSS intake, CCL3-deficient mice were injected with either HB-EGF-pLIVE or control vector at a dose of 10 μg/head by using TransIT-EE Hydrodynamic Delivery Solution. Plasma tRANTES/CCL5 levels were determined by using a commercially available ELISA kit against mouse CCL5 (R&D Systems). All animal experiments were approved by the Committee on Animal Experimentation of Kanazawa University and performed in compliance with the Kanazawa University's Guidelines for the Care and Use of Laboratory Animals.

Immunohistochemical analyses of mouse colon tissues

Resected mouse colon tissues were fixed in Tissue-Tek Ufix (Sakura Fine Technical Co.) for paraffin embedding or were immediately frozen in Tissue-Tek O.C.T. compound (Sakura Fine Technical Co.) to be stored at -80°C. Paraffin-embedded sections were cut at 3 μm thickness and stained with hematoxylin and eosin solution. In addition, 5 μm-thick sections were made and stained with Masson's trichrome solution (Sigma-Aldrich) for the detection of collagen deposition. Frozen sections were fixed in ice-cold methanol for 5 minutes for an immunohistochemical analysis. For antigen retrieval of paraffin sections, the deparafinized slides were either autoclaved in 10 mmol/L citrate buffer (pH 6.0) for 5 min at 121°C (anti-type I collagen), treated with 0.1% proteinase K solution for 15 min at 37°C (anti-Ly6C, anti-CCL3, or anti-CCR5), or treated with 0.1% trypsin solution for 15 min at 37 °C (anti-F4/80 or anti-Ly6G). Endogenous peroxidase activity was blocked using 0.3% H_2O_2 for 15 minutes, followed by incubation with Blocking One Histo (Nacalai Tesque) for 15 minutes. The sections were incubated with the optimal dilution of the antibody overnight in a humidified box at 4°C. The resultant immune complexes were then detected by the ABC Elite kit (Vector Laboratories) and peroxidase substrate 3,3'-diaminobenzidine kit (Vector Laboratories), according to the manufacturer's

instructions. Positive signals or areas were measured on 5 randomly chosen visual fields at x 100 magnification by means of Image J. For a double-color immunofluorescence analysis, Alexa Fluor 546 donkey anti-goat, Alexa Fluor 594 donkey anti-rabbit or Alexa Fluor 488 donkey anti-rat antibodies were used as secondary antibodies. Immunofluorescence was visualized on an OLYMPUS BX50/DP70. Double-color immunostaining with anti-rabbit HB-EGF and anti-rabbit type I collagen staining was conducted by using Zenon Rabbit IgG Labeling Kits (Invitrogen), according to the manufacturer's instructions.

qRT-PCR analysis

Total RNAs were extracted from the colon tissue using RNeasy Mini Kit (Qiagen). After treatment with RNase-free DNase I (Qiagen), 2 μg of total RNA was reverse-transcribed using SuperScript III First-Strand Synthesis System (Invitrogen) to obtain cDNA. qRT-PCR was performed on the obtained cDNA using StepOne real-time PCR system (Applied Biosystems) using Fast SYBR Green PCR Master mix (Applied Biosystems) and the primers listed in Supplementary Table S1. Expression levels of the target genes were analyzed through the ΔΔCT comparative threshold method. Hypoxanthine phosphoribosyl transferase (HPRT) gene or GAPDH was used as an internal control.

Determination of HB-EGF concentration in colon tissues

At the indicated time intervals, colon tissues were collected and homogenized with a lysis buffer (20 mM Tris-HCl, pH 7.6; 150 mM NaCl; 1 % Triton; and 1 mM EDTA) containing Complete Protease Inhibitor Cocktail (Roche-Diagnostics). Homogenates were centrifuged to obtain protein lysates. After determination of the protein concentration by BCA Protein Assay Kit (Pierce), the resultant protein lysates were used to determine their concentrations of HB-EGF with the help of enzyme-linked immunosorbent assay (ELISA) kit for HB-EGF (Uscn Life Science Inc.) according to the manufacturer's instructions.

Isolation of murine fibroblasts for *in vitro* culture

The colon was collected from the mice and was opened longitudinally. Then, the tissues were washed to remove fecal contents, and were shaken in HBSS containing 5 mM EDTA for 20 min at 37°C. After removing epithelial cells and fat tissue, the intestines were further cut into small pieces and incubated with Fibroblast Medium Kit (CELLnTEC) at 37°C for 3 days. Thereafter, unattached cells were removed by washing, and the medium was replaced with the same fresh medium. The cells were incubated for additional 4 days until becoming confluent. Then, the cells were detached by treatment with 0.25 % trypsin for 2–3 min at 37 °C and were split at a ratio of 1:2 or 1:3. Cells were maintained in Fibroblast Medium and subcultured every 7 to 10 days. By the third passage, the cells formed homogeneous monolayers morphologically consistent with fibroblast-like cells and were confirmed to consist of >90% type I collagen-positive cells. Colon fibroblasts were used for *in vitro* culture experiments at a confluence between the third and sixth passage.

Preparation of the fibroblast-enriched cell fraction

Colon tumor tissues were obtained from the mice at 56 days after the initiation of DSS intake and were opened longitudinally. Then, the tissues were washed to remove fecal content, and were shaken in HBSS containing 5 mM EDTA for 20 min at 37°C. After removing epithelial cells and fat tissues, the intestines were further cut into small pieces and incubated with RPMI 1640 containing 4% FBS, 1 mg/ml collagenase type I, 1 mg/ml dispase, and 40μg/ml DNase I for 1 hr at 37 °C in a shaking water bath. After being washed with HBSS containing 5mM EDTA, the tissues were resuspended in 5 ml of 40% Percoll (GE Healthcare) and were overlaid on 2.5 ml of 80 % Percoll in a 15-ml tube. After centrifugation at 2,000 rpm for 20 min at room temperature, the cells in the interface of the Percoll gradients were collected and were washed twice with PBS. The resulting single-cell suspensions were incubated with the combination of FITC-conjugated rat anti-mouse CD31 mAb (BD Biosciences) and PerCP-conjugated rat anti-mouse CD45 mAb (eBioscience,

Headquarters, USA) for 20 minutes on ice. Isotype-matched control immunoglobulins were used to detect nonspecific binding of immunoglobulin. CD31- and CD45-gated cells were sorted on a FACS Aria (BD Biosciences) as fibroblast enriched fractions.

Supplementary Figure 1 Body weight changes in WT, CCL3-deficient (CCL3KO), CCR1-deficient (CCR1KO), or CCR5-deficient (CCR5KO) mice when treated with 3.0 % DSS after AOM injection. Representative results from 5 mice are shown here. Body weight changes were calculated on the assumption that the body weight before the DSS treatment was 100 %.

Supplementary Figure 2 Body weight changes in CCL3-, CCR1-, or CCR5-deficient mice when treated with 4.5 % DSS after AOM injection. Representative results from 5 mice are shown here. Body weight changes were calculated on the assumption that the body weight before the DSS treatment was 100 %.

Supplementary Figure 3 The levels of *HGF*, *EREG*, *bFGF*, *tenascin C*, *MMP-2*, *MMP-9*, *CXCL1*, and *CXCL2* mRNA were quantified by real-time PCR on total RNAs extracted from the colon of WT (closed boxes), CCL3-deficient (open boxes), or CCR5-deficient mice (hatched boxes), and normalized to the level of HPRT mRNA. All values represent the mean + SEM (n=5 animals). *, $p<0.05$, WT vs. CCL3KO or CCR5KO.

Supplementary Figure 4 Effects on type I collagen accumulations in HB-EGF pLIVE vector treated mice. HB-EGF pLIVE vector was in vivo transduced to CCL3-deficient mice at 42 days after the initiation of DSS intake. At 56 days after the initiation of DSS intake, colon tissues were obtained to determine type I collagen-positive areas. All values represent the mean + SEM (n=5 animals). n.s., not significant.

Supplementary Figure 5 Persistent expression of a CCR5 antagonist after *in vivo* transfer of the vector. Plasma tRANTES/CCL5 levels were determined at the indicated time intervals after the vector transfer. All values represent the mean ± SEM (n=3 animals). **, $p<0.01$ vs. untreated.

References

1. Zhang G, Vargo D, Budker V, Armstrong N, Knechtle S, Wolff JA. Expression of naked plasmid DNA injected into the afferent and efferent vessels of rodent and dog livers. *Hum Gene Ther.* 1997;**8**:1763-72.
2. Zhang G, Budker V, Wolff JA. High levels of foreign gene expression in hepatocytes after tail vein injections of naked plasmid DNA. *Hum Gene Ther.* 1999;**10**:1735-7.

Supplementary Figure S1

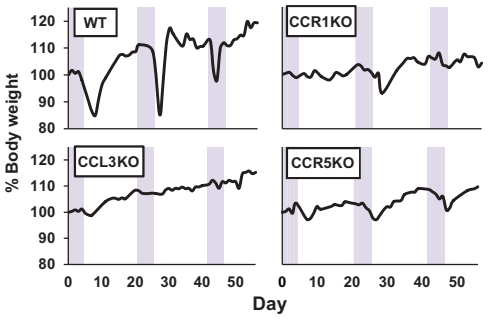

Supplementary Figure S2

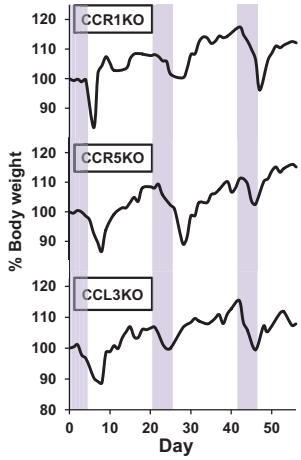

Supplementary Figure S3

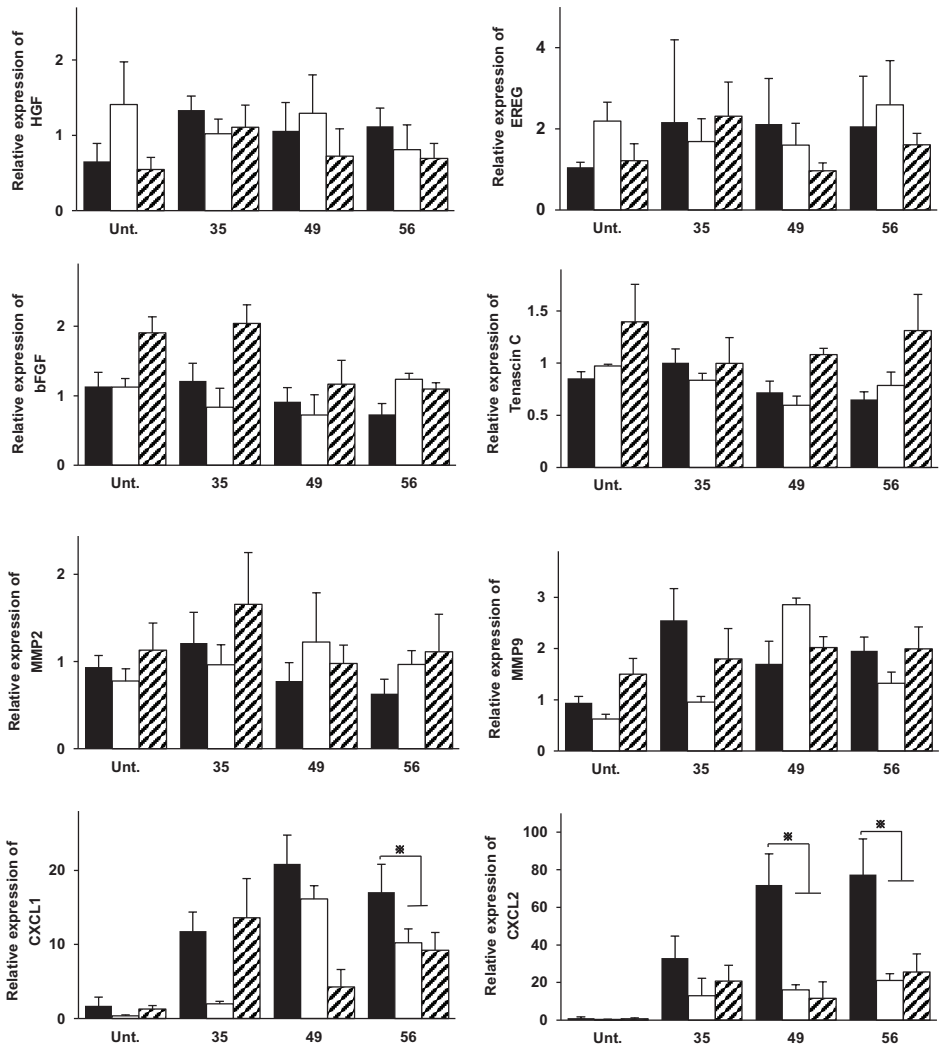

Supplementary Figure S4

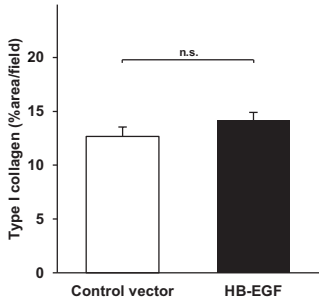

Supplementary Figure S5

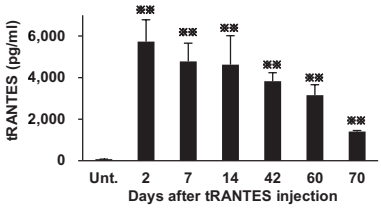

Supplementary Table S1 Sequences of primers used for qRT-PCR

Gene Name	Forward primer	Reverse primer
HPRT	tcctcctcagaccgcttt	cctggttcatcatcgctaatc
GAPDH	gcggcacgtcagatcca	catggccttccgtgtttccta
CCL3	gctgacaagctcaccctctgt	ggcagtggtggagaccttca
CCL4	cagcaccaatgggctctga	gccgggaggtgtaagagaaac
CCL5	tccaatcttgcagtcgtgtttg	tctgggttggcacacacttg
CCR1	tttgtgggtgaacggttctg	tggtatagccacatgcctttga
CCR5	catccgttccccctacaaga	ggaactgacccttgaaaatcca
Type I collagen	aggcttcagtggtttggatg	cttcacccttagcaccaactg
HB-EGF	gcaaatgcctccctggttac	ctacagccaccacagccaaga
HGF	tcggataggagccacaagga	ccgaggccagctgcaat
Tenascin C	gcaaccaaggacaatgtgtg	tgtcccatgccagatttaca
PDGFRβ	caccttctccagtgtgctga	ggagtccatagggaggaagc
bFGF	gacccacacgtcaaactacaactc	ctgtaacacacttagaagccagcag
MMP-2	tgaactgcgctgtcaatgc	cttgagagtggctatgacttctgtct
MMP-9	tccccaaagacctgaaaacct	gcccgggtgtaaccatagc
CXCL1	tgggattcacctcaagaaca	cttggggacacctttagca
CXCL2	tcaagggcggtcaaaaagtt	cctttgttcagtatcttttggatgatt
Epiregulin	taccgccttagttcagatgg	acatcgcagaccagtgtagc